Local Velocity Representation: Evidence from Motion Adaptation

Paul R. Schrater [a] and Eero P. Simoncelli [b]

[a] *Department of Neuroscience*
University of Pennsylvania
Philadelphia, PA 19104
email: schrater@psych.upenn.edu

[b] *Center for Neural Science*
New York University
New York, NY 10003
email: eero@cns.nyu.edu

8 August 1998

Abstract

Adaptation to a moving visual pattern induces shifts in the perceived motion of subsequently viewed moving patterns. Explanations of such effects are typically based on adaptation-induced sensitivity changes in spatio-temporal frequency tuned mechanisms (STFMs). An alternative hypothesis is that adaptation occurs in mechanisms that independently encode direction and speed (DSMs). Yet a third possibility is that adaptation occurrs in mechanisms that encode two-dimensional pattern velocity (VMs). We performed a series of psychophysical experiments to examine predictions made by each of the three hypotheses. The results indicate that: (1) adaptation-induced shifts are relatively independent of spatial pattern of both adapting and test stimuli, (2) the shift in perceived direction of motion of a plaid stimulus after adaptation to a grating indicates a shift in the motion of the plaid pattern, and not a shift in the motion of the plaid components, and (3) the two-dimensional pattern of shift in perceived velocity radiates away from the adaptation velocity, and is inseparable in speed and direction of motion. Taken together, these results are most consistent with the VM adaptation hypothesis.

Key words: Motion, Velocity, Adaptation, Aftereffect, Matching.
Running Head: Motion Adaptation.

Published in: Vision Research 38(24), pp. 3899–3912, 1998.

1 Introduction

The pattern of local image velocities across the retina encodes valuable information about the environment, such as direction-of-heading, and three-dimensional structure (e.g., Gibson, 1950; Koenderink & van Doorn, 1990). There is ample evidence that human observers use this information to interpret the world (e.g., Warren & Hannon, 1988). Yet the mechanisms by which the human visual system measures and represents these local velocities remains an open question in visual science.

A variety of mechanisms have been proposed for the representation of local velocity information. The most well-known are the spatio-temporal frequency mechanisms (STFMs), which are tuned for pattern orientation, spatial frequency, and temporal frequency. Abundant psychophysical evidence exists for these mechanisms, which are characterized as having half-amplitude bandwidths of roughly one octave in spatial frequency and roughly 30 degrees in orientation (for review, see Graham, 1989). Physiologically, these mechanisms have been associated with neurons in the primary visual cortex (area V1) of cats and monkeys which have similar tuning characteristics. The response of such mechanisms has been directly linked to the local velocity of a moving pattern (Movshon *et al.*, 1986). In particular, the power spectrum of a translating pattern lies on a plane in the spatio-temporal Fourier domain (Watson & Ahumada, 1983), and the tilt and orientation of this plane specify the translation velocity. Thus, a subset of STFMs whose frequency tuning regions intersect the plane will respond to such a stimulus, and their pattern of response might serve to implicitly encode the stimulus velocity.

It is important to note, however, that STFMs are not *explicitly* tuned for local image velocity (Albright, 1984; Movshon *et al.*, 1986). A number of authors have suggested that local velocities might be directly represented through velocity-tuned mechanisms (VMs) that receive input from STFMs (e.g., Adelson & Movshon, 1982; Albright, 1984; Movshon *et al.*, 1986). There is physiological evidence suggesting that a subpopulation of neurons in simian visual area MT exhibit the response properties expected from velocity-tuned mechanisms: they are tuned for both speed and direction of motion[1] (DOM) (e.g., Maunsell & Essen, 1983; Albright, 1984; Rodman & Albright, 1987), are broadly tuned for spatial frequency, and receive primary input from direction-selective V1 neurons (e.g., Movshon & Newsome, 1996). These neurons respond to the *pattern* motion of a sinusoidal plaid (Movshon *et al.*, 1986). By comparison, neurons in primary visual cortex are narrowly tuned in spatio-temporal frequency and orientation, and respond to the motion of the two component gratings which constitute a sinusoidal plaid. The idea that MT neurons could compute local velocities by selectively combining V1 afferents is corroborated by several neural models (e.g., Heeger, 1987; Grzywacz & Yuille, 1990; Simoncelli, 1993; Sereno, 1993; Nowlan & Sejnowski, 1995; Simoncelli

[1] We use the phrase “direction of motion” instead of the simpler term “direction”, since this has been used throughout the literature to refer to a binary quantity (e.g., up or down).

& Heeger, 1998). The presence of such neurons in simian cortex adds plausibility to the existence of velocity tuned mechanisms in human cortex. In addition, a recent study by Yang and Blake (1994) provides psychophysical evidence for such broadband velocity-tuned mechanisms in human vision.

Finally, some authors have proposed that the encoding of local velocity might be accomplished using two sets of mechanisms, one tuned for the pattern DOM and the other for speed (e.g., Sekuler, 1990; Driver *et al.*, 1992). We refer to these as direction-speed mechanisms (DSMs). The majority of psychophysical motion experiments are designed to examine either DOM or speed independently, and thus do not address the issue of joint versus independent representation of these quantitites.

Adaptation can provide a powerful probe for exploring visual mechanisms, given a few reasonable assumptions. Suppose that the visual system represents a particular stimulus parameter using a population of mechanisms that are tuned for that parameter. Then the perceived value of that parameter is determined by the relative responses within the population.[2] Extended stimulus exposure is assumed to reduce the responsivity of the mechanisms within the population by an amount that is a monotonic function of their sensitivity to the stimulus. This change in responsivity shifts the value of the encoded stimulus parameter away from that of the adaptor. Given these assumptions, the pattern of adaptation-induced perceptual shifts should be indicative of tuning of the encoding mechanisms (e.g., Osgood & Heyer, 1952; Sutherland, 1961; Pantle, 1968; Blakemore & Sutton, 1969; Blakemore *et al.*, 1970; Coltheart, 1971; Georgeson & Harris, 1984; Graham, 1989; Ross & Speed, 1991; Snowden, 1994). For example, Blakemore *et al.* (1970) observed that the perceived spatial frequency of a sinusoidal grating is shifted repulsively away from the frequency of an adapting grating, and from this inferred the existence of visual mechanisms tuned for spatial frequency.

In this paper, we probe the representation of local velocity by examining perceptual shifts induced by adaptation to moving patterns. Although there is a large body of literature on motion adaptation effects (e.g., see Wade, 1994), only a small portion of it addresses perceptual shifts. Most perceptual shift studies have separately examined the effects of motion adaptation on perceived DOM, temporal frequency, or speed. DOM repulsion has been reported by Levinson and Sekuler (1976) . Mather (1980) subsequently explained this result via adaptation of STFMs. However, because of the stimuli employed in these previous studies (translating random dots for both adaptation and test stimuli), the three motion encoding schemes described above make qualitatively similar predictions about the expected shifts in perceived DOM.

[2] We are intentionally non-specific regarding the rule for "reading" the population. Example rules are a maximum ("winner-takes-all"), and the population mean (in which the population response is interpreted as a discrete probability density over the stimulus parameter).

Other authors have examined shifts in perceived speed. Clymer (1973) reports that test speeds are repulsed away from the adaptation speed. Thompson (1980) and Smith (1985) report that adaptation always decreases perceived test speed, while Smith and Edgar (1994) report repulsion of perceived speed for some combinations of adaptor and test. Thompson explained his data using speed-tuned mechanisms, but many authors have interpreted their results using STFMs (e.g., Sekuler *et al.*, 1978; Smith, 1987; Smith & Edgar, 1994). Again, the three encoding schemes described above cannot be distinguished on the basis of these studies.

The purpose of our experiments is to determine whether adaptation of one of the three mechanisms described above can account for the perceptual shifts arising from motion adaptation to different stimuli. Portions of this work have been presented in (Schrater & Simoncelli, 1994; Schrater & Simoncelli, 1995). In the first experiment, we examine shifts in perceived DOM resulting from adaptation to moving patterns. We find that adaptation to sine gratings and drifting random dots produces nearly the same perceptual shifts in DOM of sinusoidal test stimuli. We also find that changes in spatial frequency of test stimuli of up to two octaves have a minimal effect on the magnitude of perceptual shifts. Both of these results are inconsistent with a simple form of STFM adaptation, since STFMs are assumed to be pattern-specific with roughly octave-bandwidth frequency tuning.

In the second experiment, shifts in perceived DOM of a sinusoidal plaid pattern are examined after adaptation to a grating. The plaid stimuli are constructed such that adaptation of STFMs should produce opposite shifts in perceived DOM, compared with adaptation of VMs or DSMs. Again, the results are inconsistent with adaptation of STFMs.

Finally, in order to address the predictions made about the joint encoding of speed and direction by the VM and the DSM hypotheses, a novel two-dimensional matching procedure is used to measure vectorial shifts in perceived velocity of drifting dot patterns. We find that perceived velocities are shifted repulsively away from the adapting velocity, and that these shifts are not separable in speed and DOM. This result is inconsistent with adaptation of DSMs. All three experimental results can be explained as resulting from adaptation of mechanisms tuned for two-dimensional image velocity.

2 General Methods

2.1 Apparatus

Stimulus displays were generated on a Macintosh Centris 650 computer using custom software based on Denis Pelli's VideoToolbox routines and displayed on a 21" RasterOps monochrome monitor. The monitor has a P104 phosphor, a vertical re-

fresh rate of 75 Hz, a maximum luminance of 88 cd / m^2, and was calibrated and gamma-corrected. Subject viewing distance was fixed at 61 cm and head position was stabilized using a chin rest. At this distance, monitor pixels had a width (and height) of 0.034 degrees. Subject fixation was monitored informally by the experimenters. In addition, subjects were instructed not to enter a response for trials in which they felt they had moved their eyes.

2.2 Stimuli

Stimuli consisted of translating sinusoidal gratings, plaids, or random dot patterns. All stimuli appeared within circularly symmetric spatial windows. Both spatial window and temporal onset and offset boundaries were smooth, following a profile specified by:

$$a(r) = \begin{cases} 1, & r < w \\ 0, & r > w + t \\ \cos^2[\pi(r - w)/(2t)], & \text{otherwise}, \end{cases}$$

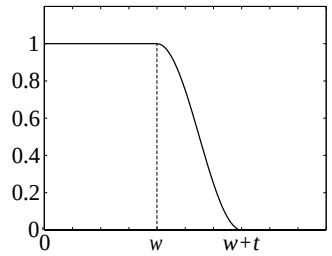

Sinusoidal grating and plaid animation was performed by colormap lookup table (CLUT) animation. Sinusoidal stimuli used the entire 8-bit CLUT (256 gray shades linearly spanning their luminance range). For plaid stimuli, each component grating was assigned to half the pixels (spatially interleaved in a checkerboard pattern) and half of the 8-bit CLUT range, allowing independent animation of each component.

Translating dot stimuli were animated using vertical blanking interrupt cinematography. In experiments 1 and 2, dots were one pixel in size and 10% of the dots were placed in random spatial coordinates on the first frame. For each subsequent frame, dot positions were advanced by integer amounts. Dots translating beyond a display boundary reappeared at the opposite boundary, so as to maintain constant dot density.

For experiment 3, finer control of translating dot velocities was needed. Subpixel displacements were achieved using a subsampling method. A 240×240 pixel image of a Gaussian with standard deviation $\sigma = 30$ was bandlimited to a frequency of $\pi/40$ radians / pixel. Because of this bandlimiting, this image could be subsampled by a factor of 40 without spatial aliasing. Shifting the origin of the subsampling lattice produces dot displacements in increments of 1 / 40th pixel. The subsampled dot images (size 6×6 pixels) are inserted additively into each movie frame at the appropriate locations. In addition, dot density for experiment 3 was 4% (instead of 10%), but otherwise dot animation was the same as described above for the first

two experiments.

2.3 Subjects

There were 5 naive subjects (IT, RV, RLY, LG and SO) with normal or corrected-to-normal vision. Subjects were chosen without regard to gender, race, or ethnicity and were monetarily compensated for their participation. The two authors also participated as subjects. PRS has (corrected) normal vision, while EPS has (corrected) normal vision in the right eye. All subjects viewed stimuli binocularly except EPS, who viewed monocularly.

3 Experiment 1: Shifts in Apparent DOM of Sinusoids

STFMs are sensitive to changes in spatial pattern, and thus one expects that adaptation effects arising from STFMs should depend on the spatial pattern of the adaptor. The purpose of this experiment was to test this prediction, and to provide control conditions for experiment 2. We measured shifts in perceived DOM for test gratings of several different spatial frequencies after adaptation to either drifting random dot fields or drifting gratings of a fixed spatial frequency. The STFM adaptation hypothesis predicts that the magnitude of the shifts in DOM should fall off as the difference between adapting and test spatial frequencies increases.

3.1 Methods and Procedure

Subjects viewed an initial adaptation stimulus drifting upward at 2.7 deg/sec for a period of 60 sec. Each subsequent trial consisted of re-adaptation to this stimulus (10 sec), a blank interval (0.5 secs), presentation of a drifting sinusoidal test stimulus (0.7 secs), and a response period (1 sec). During the response period, the subject adjusted the direction of a white arrow to indicate the perceived direction of motion. If the subject did not respond in the allotted time period, the trial was discarded and the stimulus was re-shuffled into the list of remaining trials. The use of a fixed response period ensures a constant adaptation state.

Adaptation stimuli were either drifting sinusoidal gratings (spatial frequency 1.4 cyc/deg) or rigidly translating random dot patterns. Test stimuli were drifting sinusoidal gratings of variable spatial and temporal frequency. The aperture window had a radius of $r = 3.4$ degrees, with transition width $t = 0.17$ degrees. A black fixation cross was shown at the center of the aperture window. Stimulus onset and offset transition durations were $t = 0.095$ seconds. The Michelson contrast of all stimuli was 0.4, and the background luminance of the screen was fixed at half the maximum luminance.

For each choice of adapting stimulus, all trials (including those with different test spatial frequencies) were randomly intermixed. A rest period of 10-15 minutes was imposed between blocks having different adaptation stimuli. Prior to any data collection, each subject was given 30 minutes of pre-experimental pointer adjustment training with feedback and no adaptation. These pre-adaptation trials indicated no significant pre-adaptation biases in perceived DOM. No feedback was given during adaptation trials.

3.2 Results

Figure 1 shows results for four subjects. The graphs show the shift in perceived DOM as a function of test DOM (relative to adapting DOM). DOM shift was computed as the difference between the observer's indicated DOM and actual DOM. Thus, a point above the X-axis indicates that the perceived DOM was shifted clockwise relative to the actual DOM. Points lying on the horizontal axis may be classified based on the slope of the curve: A positive slope corresponds to a "repulsive" DOM, and a negative slope indicates an "attractive" DOM. The line style indicates the adapting stimulus type: Solid lines correspond to sine gratings, and dashed lines to random dot patterns. To quantify differences between the two curves, a one-way multivariate analysis of variance (MANOVA) was computed for each observer on the curve segments from test DOM -90 deg to +90 deg. This test indicates that the curves resulting from grating and dot adaptation are not significantly different for 3 of 4 observers. Figure 2 shows DOM shifts measured with a slower test speed of 1.0 deg/sec. These data were used to generate predictions for Experiment 2, and are quite similar to those of Fig. 1.

We also examined the dependence on test spatial frequency (for sinusoidal test stimuli, with speed 2.7 deg/sec). Average shift as a function of test spatial frequency is plotted in Fig. 3. The adaptation spatial frequency was constant at 1.4 cyc/deg, while test spatial frequency covered a range from 0.5 to 4.2 cyc/deg. Average shift was computed from the full shift curves (as shown in Fig. 1) by averaging the absolute value of the 6 data points in the range -56 to 56°. Figure 3 also includes an analysis of variance computed on the data for each observer, which indicates an insignificant spatial frequency effect for three of the four observers.

3.3 Discussion of Experiment 1

These data clearly show that the adaptation DOM is repulsive. The magnitude of this repulsion is maximal approximately 30 deg from the adaptation DOM. The data also show a similar but smaller repulsion away from the direction opposite to the adaptation DOM (i.e., "antipodal" repulsion). Between these two repulsive points, there is an attractive point rougly 100-120 deg away from the adaptation

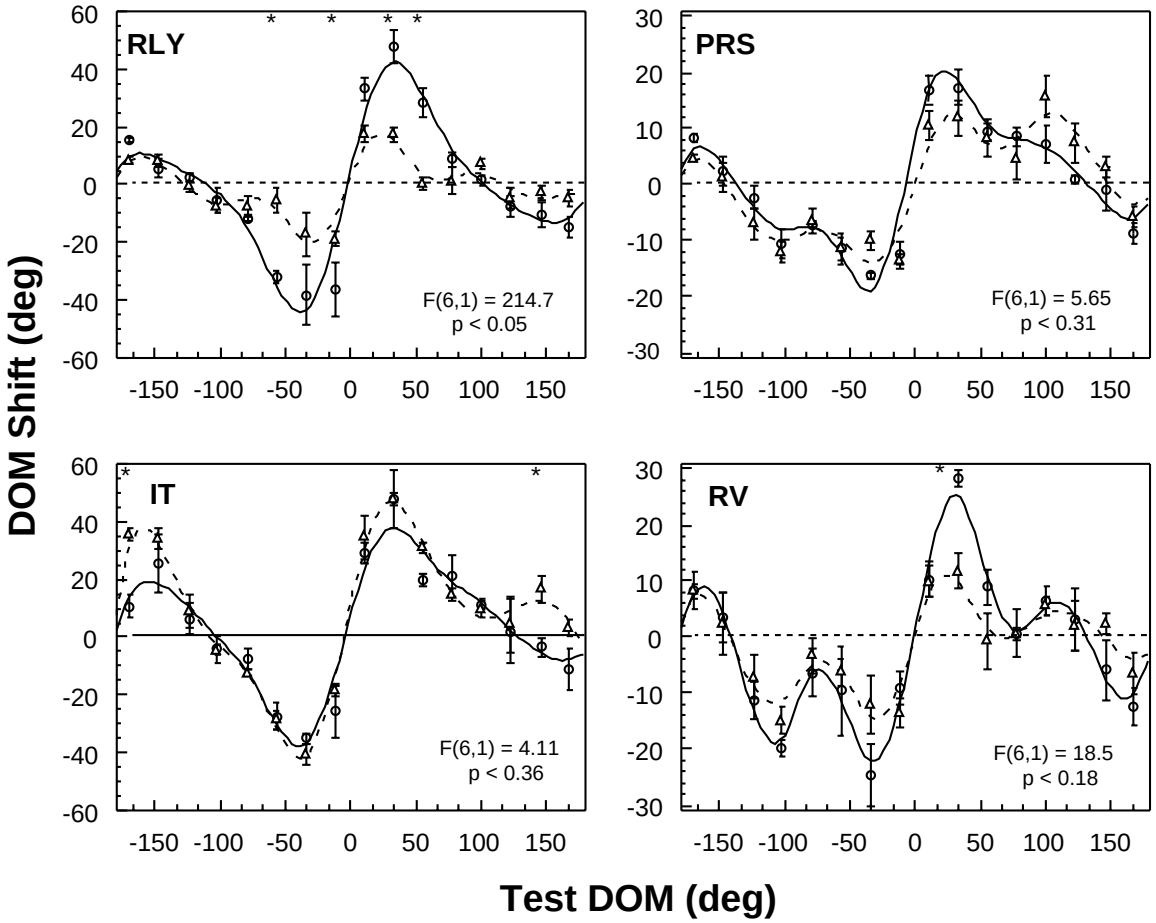

FIGURE 1. Adaptation-induced shift in the perceived DOM of test gratings as a function of their veridical DOM. Adaptation stimuli were either drifting sinusoidal gratings (continuous lines) or drifting random dots (dashed lines). Test and adapting stimulus speeds were 2.7 deg/sec. Each point represents an average of four trials; error bars indicate standard error. Smooth curves are the least-squares fits of the data with a four-term Fourier series. Asterisks indicate those data points for which the shift measured under the two adaptation conditions was statistically different ($p < 0.05$, T-test). MANOVA results are recorded in the lower right hand corner of the graphs.

DOM. The repulsive behavior is seen to be similar for both grating and random dot adaptors.

Repulsive DOM shifts have been previously reported for translating dot stimuli (Levinson & Sekuler, 1976), and also for translating sinusoidal stimuli (Lew *et al.*, 1991). The shifts shown in Fig. 1 are similar, but the magnitude of the effect reported here is much larger. In particular, Levinson and Sekuler find maximal shifts of roughly 12 deg, whereas the shifts plotted in Figs. 1 and 2 show maximal values in the range of 24-50 degs. It seems likely that this is due to a difference in re-adaptation duration: Levinson and Sekuler used re-adaptation periods of 3 sec, whereas the current study used periods of 10 sec.

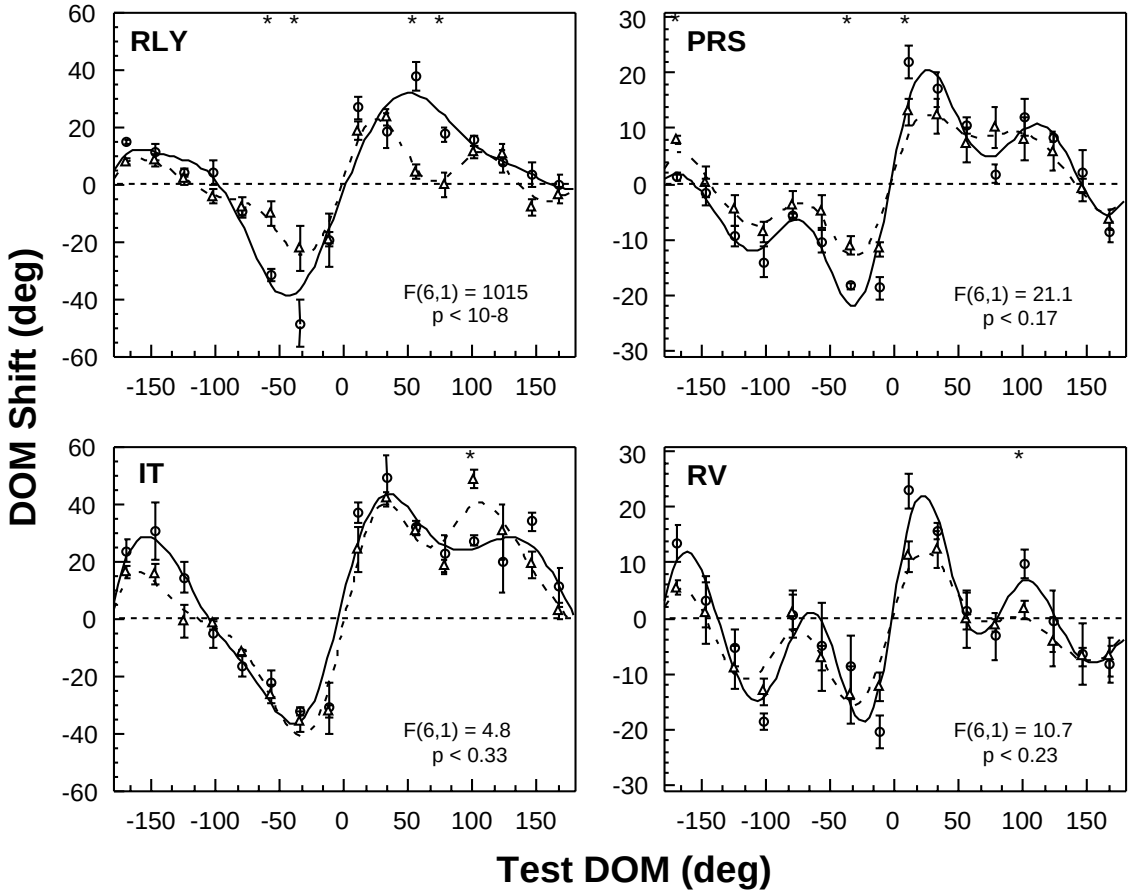

FIGURE 2. Shift in DOM for slower (1.0 deg / sec) test grating. See Fig. 1 for details.

In addition, these previous investigations did not report antipodal repulsion as seen in our data. We hypothesize that the use of sinusoidal stimuli in our experiments may lead to a combination of static orientation (i.e., "tilt" aftereffect) and motion adaptation effects. Orientation adaptation would be expected to produce antipodal repulsion as well as repulsion from the adaptation direction. Judging from the relative sizes of adaptation and antipodal repulsion, it seems that any contribution of static orientation adaptation to the observed perceptual shifts is small relative to motion adaptation. The phenomenal appearance of the maximally direction-shifted test gratings is consistent with this: they appear to move in a direction strikingly different from their normal direction. In addition, the hypothesis is contradicted by the observation that grating and translating dot patterns produced similar curves, even though the dot stimuli are spatially isotropic and would not be expected to produce such a tilt aftereffect.

Most importantly, the data of Fig. 3 contradict the STFM hypothesis, which predicts that the DOM shifts should decrease as the difference between adaptation and test spatial frequencies increases. Our data are consistent with those of (Thompson, 1980), which show that adaptation-induced shifts in perceived speed of gratings are not strongly dependent on spatial frequency. In addition, Ashida and Osaka (1994) found negligible spatial frequency specificity for MAEs measured us-

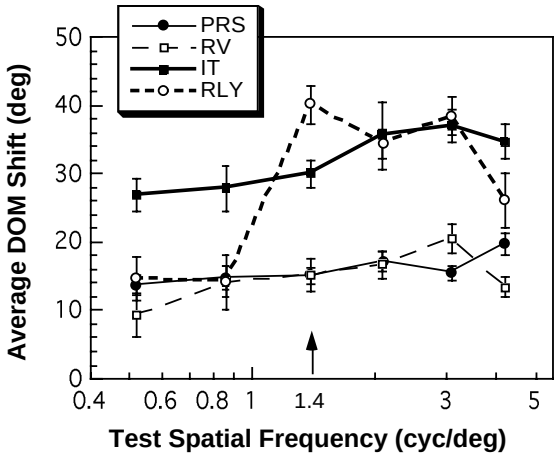

Subject	F-ratio	p
PRS	$F(5, 138) = 1.91$	$p < 0.11$
RV	$F(5, 138) = 1.95$	$p < 0.09$
IT	$F(5, 138) = 1.94$	$p < 0.09$
RLY	$F(5, 138) = 15.80$	$p < 0.001$

FIGURE 3. Left: Average shift in DOM as a function of test spatial frequency for four subjects. The adaptation spatial frequency (arrow) was 1.4 cyc / deg, while test spatial frequency covered roughly three octaves (0.5 - 4.2 cyc / deg). Average shift was computed from DOM shift curves of Figs. 1 and 2 by averaging the absolute value of the 6 data points from -56 to 56 deg. **Right:** Analysis of variance for these data indicates no significant dependence of average shift on spatial frequency for three of the four subjects.

ing counterphase flickering test stimuli. We note, however, that spatial frequency tuning has been observed in MAE experiments using *stationary* test stimuli (Over *et al.*, 1973; Cameron *et al.*, 1992; Ashida & Osaka, 1994). We return to this issue in the *Discussion.*

4 Experiment 2: Shifts in Apparent DOM of Plaids

In the second set of experiments, we examined predictions made by the STFM adaptation hypothesis regarding perceived DOM of a test plaid after adaptation to a drifting grating. The physical DOM of a plaid stimulus can be calculated from the physical motions of its components using the "intersection-of-constraints" (IOC) construction (Adelson & Movshon, 1982). Although there are numerous situations in which the percept of plaid velocity deviates from this idealized construction, the perception of the symmetric plaids used in this experiment is well-described by the IOC DOM.

Under the VM or DSM adaptation hypotheses, adaptation causes changes in the sensitivity of mechanisms that encode the DOM of the plaid pattern. These hypotheses predict plaid pattern DOM should always be repulsed *away* from the adapting DOM, similar to the data shown in Experiment 1.

Under the STFM hypothesis, adaptation to a drifting grating will suppress the response of those STFMs tuned for the grating orientation, period and speed. This

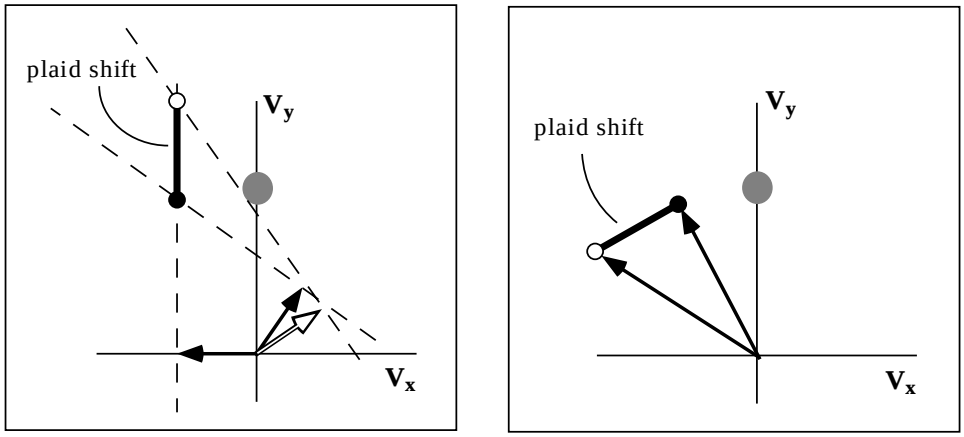

FIGURE 4. Qualitative predictions of shift in apparent plaid velocity for different adaptation hypotheses. The adaptor is an upward drifting grating with velocity indicated by the large gray circle. In both panels, arrows indicate encoded quantities, filled circles correspond to pre-adaptation percepts, and hollow circles correspond to post-adaptation percepts. **Left:** Prediction of the STFM hypothesis. Arrows indicate the perceived plaid component (normal) velocities. The normal velocity of one of the components is shifted away from that of the adapting grating (hollow arrow). The other component is not affected. The dashed lines are the "velocity constraint lines", which indicate the set of velocities consistent with each component. The perceived plaid velocity is the intersection of these constraint lines. The result of the adaptation is that the plaid DOM is shifted *toward* the adaptation DOM. **Right:** Prediction of the VM and DSM adaptation hypotheses. Arrows indicate perceived plaid velocity. The plaid pattern DOM is shifted *away* from the adaptation DOM.

would cause a shift in the encoding of the *component* velocities of a subsequently viewed plaid. Assuming that the velocity percept is determined from the encoded component velocities using an IOC construction, one would expect the perceived velocity of the plaid to match the IOC velocity of the *shifted* components.

For certain component grating configurations, the STFM hypothesis makes opposite predictions about DOM shift from the VM or DSM hypotheses. Such a configuration is illustrated in Fig. 4. In the left panel, one component grating is unaffected and the other is shifted away from the adapting DOM. Thus, the IOC velocity of these modified components is shifted *toward* the adaptor DOM. The following experiments are designed to examine such configurations.

4.1 Methods and Procedure

Methods are the same as those of experiment 1. The adaptation stimulus was a sinusoidal grating moving upward at 2.7 deg/sec. The test stimulus was a plaid composed of two sinusoidal components with normal directions differing by 135 degrees. This angle was chosen to approximately maximize the shift in one component when the shift in the other component is zero, as depicted in Fig. 4. The components moved at a speed of 1.0 deg/sec producing a coherent plaid motion

Subject	F-ratio	p
RLY	$F(16,4) = 71.6$	$p < 0.0004$
PRS	$F(16,4) = 5.29$	$p < 0.06$
IT	$F(16,4) = 4.36$	$p < 0.08$
RV	$F(16,4) = 2.61$	$p < 0.18$

Table 1: MANOVA analysis on the data from Figs. 1, 2 and 5.

of 2.7 deg / sec. All grating spatial frequencies were fixed at 1.4 cyc / deg.

4.2 Results

The results of the experiment are summarized in Fig. 5. The solid lines show the perceived shift in the plaid DOM. The plaid DOM is clearly repulsed from the adaptation DOM, in a manner similar to the results of experiment 1. The dashed lines in Fig. 5 show the shift predicted by the STFM hypothesis, computed by applying the IOC construction to the data of experiment 1 (i.e., the solid curves in Fig. 2). Since we are using symmetric plaids, the IOC DOM is simply the average of the component DOMs, and the predicted shift in plaid DOM is therefore the average of the shift in DOM of the two component gratings:

$$\Delta\theta_p(\phi) = [\Delta\theta_g(\phi - 67.5) + \Delta\theta_g(\phi + 67.5)]/2,$$

where ϕ is the physical plaid DOM (relative to the adaptation DOM), $\Delta\theta_g$ is the shift in perceived grating DOM (from experiment 1, Fig. 2), and $\Delta\theta_p$ is the predicted shift in perceived plaid DOM. These STFM hypothesis predictions are directly in opposition to the observed shifts for all four observers.

The curves for plaid test stimuli are quite similar to those obtained with grating and dot test stimuli (see Fig. 1). To quantify this similarity, a MANOVA was performed on the data points from -90 deg to 90 deg for the five curves plotted in Figs. 1, 2 and 5. The results are shown in Tbl. 1. RLY is the only subject exhibiting significant differences, and in this case it is the grating adaptation curve (Fig. 1) that differs. The dot adaptation and plaid adaptation curves are not significantly different.

4.3 Discussion of Experiment 2

The results of experiment 2 match the predictions of both the VM and DSM adaptation hypotheses, but are inconsistent with the STFM adaptation hypothesis. Our

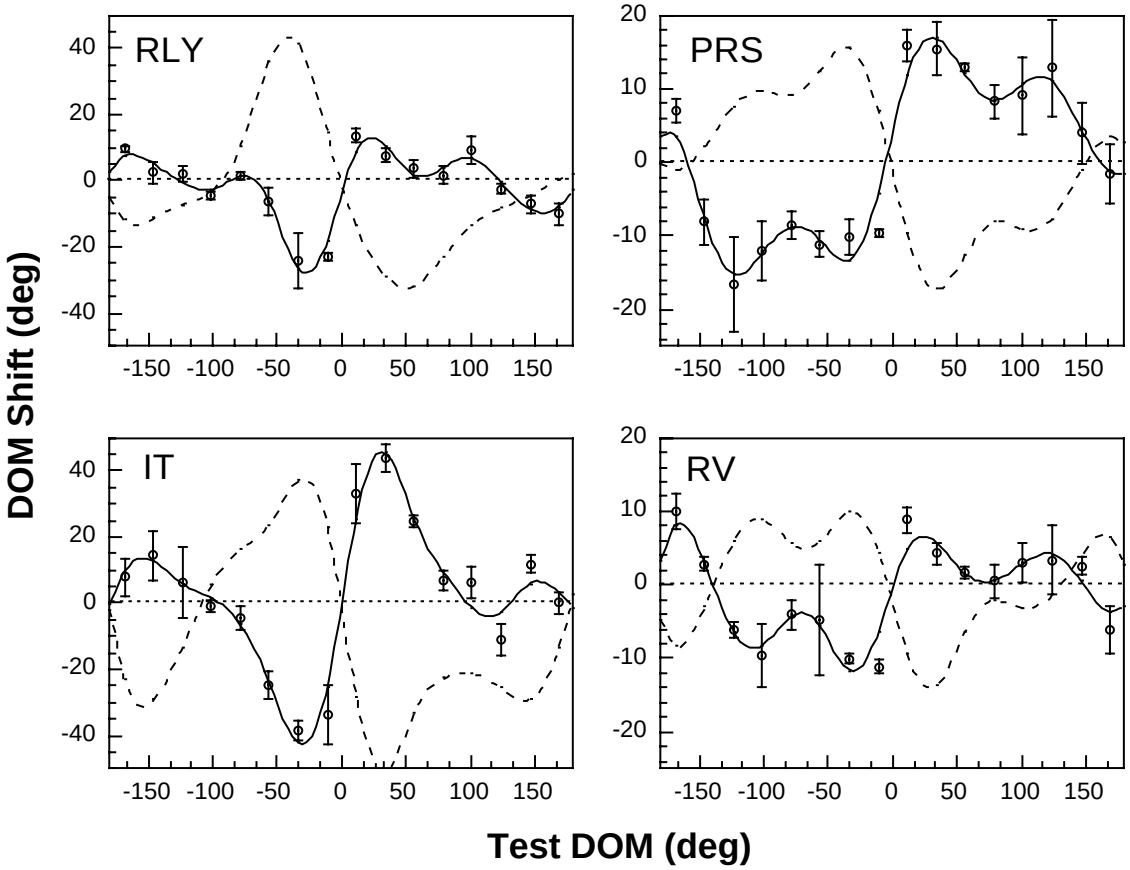

FIGURE 5. Shift in perceived DOM of test plaids as a function of their DOM. Adapting stimuli were drifting sinusoidal gratings. Solid curves are fits of the data with four Fourier harmonics. The dashed curves represent the prediction of the STFM hypothesis, computed as the IOC solution assuming component shifts of experiment 1 (Fig. 2).

data contradict the conclusions of Derrington and Suero (1991) who performed a similar experiment using a test plaid at a single DOM with a plaid angle of 90 degrees. Observers adapted to a sinusoidal grating, and were tested with a sinusoidal plaid stimulus. The adapting grating had the same orientation as one of the plaid components, but a higher speed. The data show a shift in the perceived plaid DOM away from the adapting grating DOM. Derrington and Suero interpreted this as evidence for STFM adaptation: adaptation caused a reduction in the encoded speed or temporal frequency of one of the component gratings.

Note, however, that the VM hypothesis predicts a similar shift in DOM for this test stimulus configuration, as illustrated in Fig. 6. On the left is the prediction of the STFM adaptation hypothesis. The encoded speed of the component aligned with the adaptor is reduced, and the IOC velocity of the plaid is shifted away from that of the adaptor. The right portion of the figure indicates the prediction of a VM hypothesis: again, the plaid DOM is shifted away from that of the adaptor. Thus, the Derrington and Suero data do not distinguish between these hypotheses.

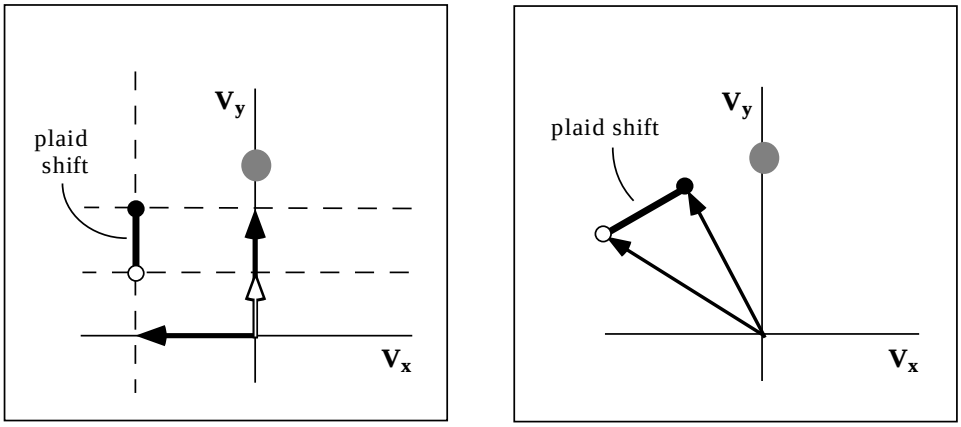

FIGURE 6. Qualitative predictions for the Derrington and Suero experiment, for different adaptation hypotheses. Filled circles correspond to pre-adaptation percept, and hollow circles correspond to post-adaptation percept. **Left:** Prediction of the STFM hypothesis. **Right:** Prediction of the VM or DSM hypothesis. See caption of Fig. 4 for further details.

This does, however, raise the question of whether component speed shifts might explain our data. In order to test this possibility quantitatively, we used the IOC construction to compute component speed shift curves which best fit the data of Experiment 2, assuming no shift in component DOM. The fitting was achieved numerically, using the Broyden-Fletcher-Goldfarb-Shanno variable-metric minimization algorithm and a least-squares error measure (Press *et al.*, 1988). The resulting component speed shift curve, averaged across subjects, is shown in Fig. 7. This is compared to perceptual speed shift data reported in Smith and Hammond (1985). It is clear that the two functions differ markedly. The fitted curve predicts that test gratings moving in the same or opposite DOMS from the adaptor should appear significantly slower, but that test gratings in other directions should appear much faster. The Smith and Hammond data show that test gratings at all DOMS appear slower, with the largest effect (about 50%) occurring when the test moves in the same DOM as the adaptor. Inclusion of the component DOM shifts can only make this worse, since these act to produce plaid DOM shifts that are opposite of those observed (see Fig. 5).

5 Experiment 3: Measurement of Two-dimensional Velocity Shifts

The results of the previous experiments provide evidence against the STFM hypothesis, and are consistent with both the VM and DSM hypotheses. In this experiment, we examine an important prediction of the VM hypothesis. If the visual system uses mechanisms which jointly encode speed and DOM, then adaptation to a stimulus with a unique velocity should induce a pattern of velocity shifts that radiate away (in both speed and DOM) from the adaptation velocity. The DSM hypothesis also predicts repulsive shifts in both speed and DOM, but in addition predicts that these shifts should be separable. That is, shifts in perceived test speed

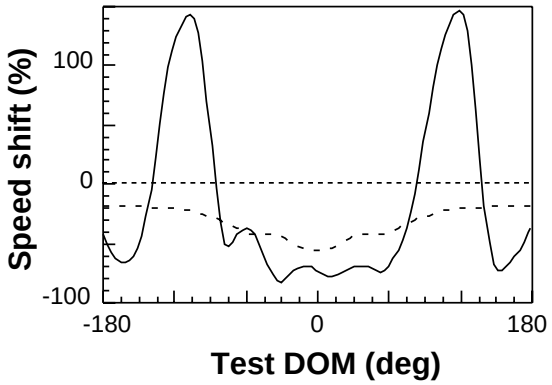

FIGURE 7. Comparison of inferred speed shift curve with a published speed shift curve. The solid line indicates the shift in component speed which best explains the plaid data of Fig. 5 (in the least square sense), averaged across the four subjects. The dashed line is an perceptual speed shift curve replotted from Smith and Hammond (1985).

should be independent of test DOM, and shifts in perceived test DOM should be independent of test speed. Smith and Hammond (1985) showed that speed shifts depend on DOM, providing some evidence against the DSM hypothesis. In the following experiment, we use a novel technique to measure the two-dimensional pattern of shifts induced by velocity adaptation, and examine the separability of this pattern.

5.1 Experimental Design

We used a matching technique to measure two-dimensional shifts in velocity. Subjects compared a test stimulus to a match stimulus that was offset both spatially and temporally. The spatial separation was chosen to be large enough to ensure that the perception of the match stimulus was not affected by the adaptation. We used the procedure of experiments 1 and 2 to measure the spatial extent of adaptation in one observer. Using an adaptation aperture of radius $r = 1.125$ deg, we examined DOM shifts in test stimuli spatially displaced between 0.5 and 6 deg from the adaptation site. The shifts essentially disappeared when the test and adapt patches had no overlap. We chose a 4.46 deg distance between the centers of the two stimulus apertures.

The test and match stimuli were temporally separated by a 0.5 sec blank interval, because the perceived motions of simultaneously presented stimuli can be shifted by the presence of the other (e.g., Loomis & Nakayama, 1973; Murakami & Shimojo, 1993). Such “motion induction” effects could be confounded with shifts due to adaptation. We chose an interval of 0.5 sec for the blank period.

Since it is difficult for subjects to simultaneously compare relative speed and DOM, we developed a novel two-step matching task. Our pilot experiments showed that DOM judgments are largely independent of the relative speeds of test and match

stimuli, but speed judgments are less accurate when the test and the match have different DOMs. Thus, as a first step we estimate perceived DOM by comparing test and match stimuli moving at the same physical speed. In the second step, we estimate perceived speed using a match stimulus with the DOM determined from the first step. Both perceived speed and DOM were measured using a two-alternative forced-choice (2AFC) procedure. Estimates of perceived values were inferred from the "point of subjective equality" (50% performance) in the discrimination task. Because of the temporal and spatial asymmetry in the test and match stimuli presentations, we could not assume that the unadapted motion percepts were veridical. Thus, perceived speed and DOM were measured both in adapted and unadapted conditions. All perceptual shifts are computed by comparison of the perceived values in the two conditions. The entire procedure is illustrated on the left side of Fig. 8.

5.2 Methods and procedure

The adaptation, test, and match stimuli in this experiment were drifting anti-aliased random dot patterns, as described in Sec. 2. The adaptation stimulus moved upward (i.e., DOM = 90 deg) at 3.9 deg/sec and always appeared in an aperture of radius $r = 1.125$ deg, with a transition width of $t = 0.17$ deg, centered 2.23 deg to the left of the fixation point. Stimulus onset and offset transition durations were $t = 0.067$ seconds. In order to avoid unequal contrast adaptation on the two sides of the fixation dot, a spatially and temporally random white noise pattern with the same contrast as the adaptation pattern was presented 2.2 deg to the right of the fixation dot during adaptation periods.

An initial adaptation period of 1 minute was followed by a block of trials. Each trial began with a re-exposure to the adaptation stimulus for 4 sec. The trial protocol is depicted in the right side of Fig. 8. For speed discrimination trials, observers indicated the interval containing the faster stimulus (by pressing one of two keys). For DOM discrimination trials, observers were asked to choose the interval containing the stimulus which appeared to move in a more counter-clockwise direction. If subjects did not respond within the allocated response time (0.75 sec), they were notified with a beep, and the trial was re-shuffled into the block.

Trials were grouped into three blocks. The first block consisted of DOM comparisons for those test velocities with DOM shifts. The second block contained the speed comparisons for these test velocities. The third block contained speed comparisons for upward- and downward-moving test velocities, for which DOM comparisons were not made. For each block, the order of presentation of test stimuli was randomized, and the match stimulus parameter was controlled using a QUEST procedure (Watson & Pelli, 1983) that tracked the 50% performance level.

Observers were given 1 hour of training with feedback, after which the task was

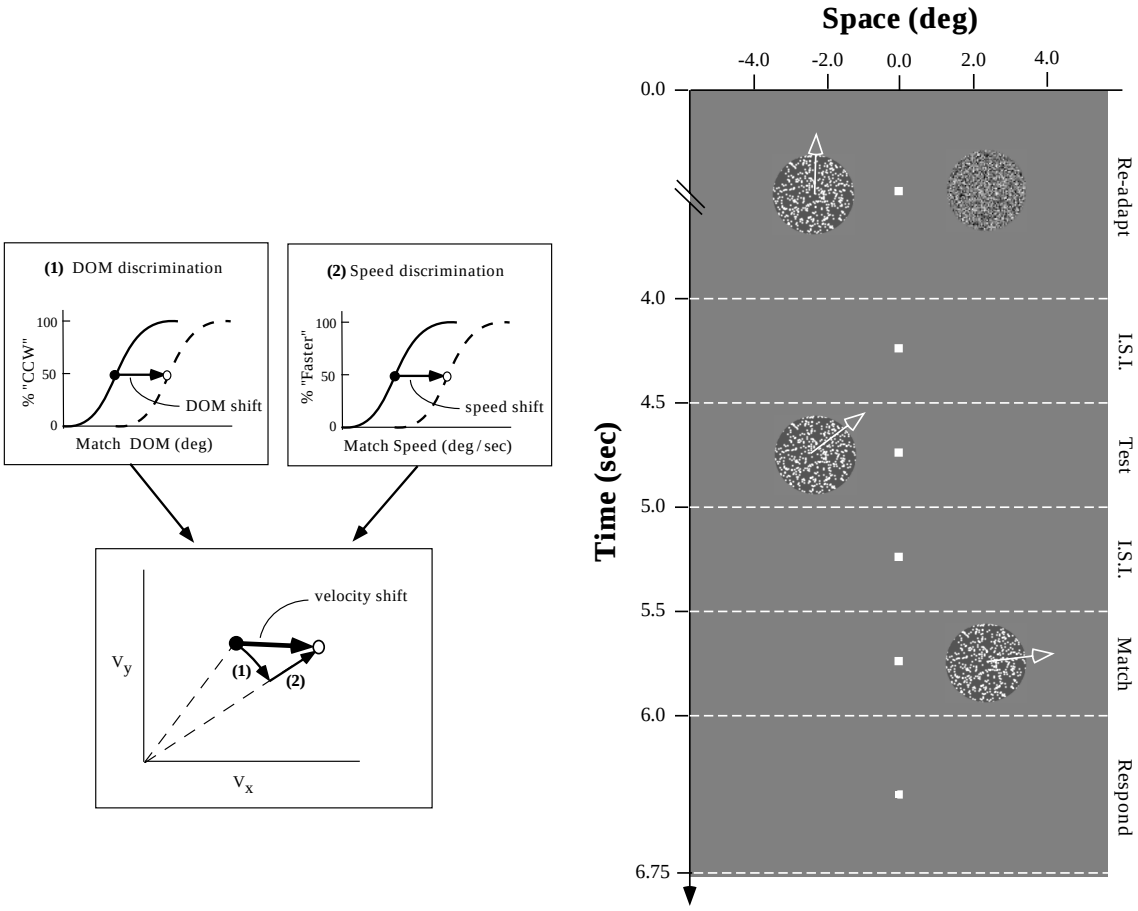

FIGURE 8. Left: Two-step procedure for measuring velocity shifts. In step 1, the DOM shift is measured using a match stimulus with the same physical speed as the test stimulus. Hollow circle indicates the matching pre-adaptation DOM, filled circle indicates the matching post-adaptation DOM. In step 2, the speed shift is measured similarly, using match stimuli with DOMs set to the perceived (shifted) DOM estimated in step 1. These two shifts correspond to the components of the total (vectorial) shift in velocity, as reported in Fig. 9. **Right:** Graphical depiction of the experimental protocol. See text for further details.

performed without feedback. Within each session, the observer performed the task twice without adaptation and once with adaptation, for 2-3 sessions. Since the two naive subjects showed higher between-session variability than within-session variability, shifts were computed within a session and averaged across sessions.

5.3 Results

The experimental results are plotted in Fig. 9, which shows shifts in the two-dimensional space of stimulus velocity. Velocity shifts were computed as described in Fig. 8. Data were only collected for test velocities in the right half plane, with these shifts symmetrically replotted in the left half plane to simplify interpretation.

Radial (speed) and angular (DOM) standard errors are indicated with grey boxes for the data in the right half plane. Angular errors is calculated using as follows:

$$r = \sum_{j=1}^{N} \exp(i\theta_j)/N$$
$$S_\theta^2 = 2(1 - |r|)/N,$$

where the θ_j's are the DOM shifts measured on individual trials. The mean direction is given by the angle (complex phase) of r, and the standard error S_θ is related to the length (magnitude) of r. These expressions converge to the normal standard error for small angular deviations, and standard errors computed by both methods are quite similar for the data reported. Note that for our data, these standard errors are quite small (typically a few degrees).

The main feature of the data in the upper half plane is the strong two-dimensional radial repulsion of the perceived motion of the test velocities away from the adaptation velocity. The shifts in the lower half plane are much smaller on average (in fact, they are often statistically insignificant), and no consistent pattern across subjects is evident.

To directly examine the question of separability, we re-plot some of these data in figure 10. The left side of the figure shows DOM shifts re-plotted for two test speeds at a fixed test DOM of 82 deg. These shifts vary significantly with test speed. The right side shows the speed shifts re-plotted for two test DOMs, at a fixed test speed of 4.5 deg / sec. For 3 of 4 observers, these shifts vary significantly with test DOM. EPS shows no significant change in speed shift for the two points re-plotted here, but does show significant changes in speed for other points.

5.4 Discussion

The data of Fig. 9 demonstrate that adaptation to moving stimuli induces repulsive shifts of perceived velocity away from the adaptation velocity, thus generalizing the DOM repulsions observed in experiments 1 and 2. This two-dimensional radiating pattern of velocity shifts is consistent with the VM hypothesis, in which velocity is encoded by a population of mechanisms that are jointly tuned for speed and DOM. The data, as re-plotted in Fig. 10, are clearly not separable and are thus inconsistent with the DSM hypothesis, which predicts that DOM shifts should be independent of test speed, and that speed shifts should be independent of test DOM.

Analogous patterns of two-dimensional repulsive shifts have been observed in saccadic eye displacements, following reversible chemical lesions in primate Superior Colliculus (Lee *et al.*, 1988). Neurons in this area are known to be tuned for the two-dimensional displacement incurred during a saccadic eye movement. The lesion

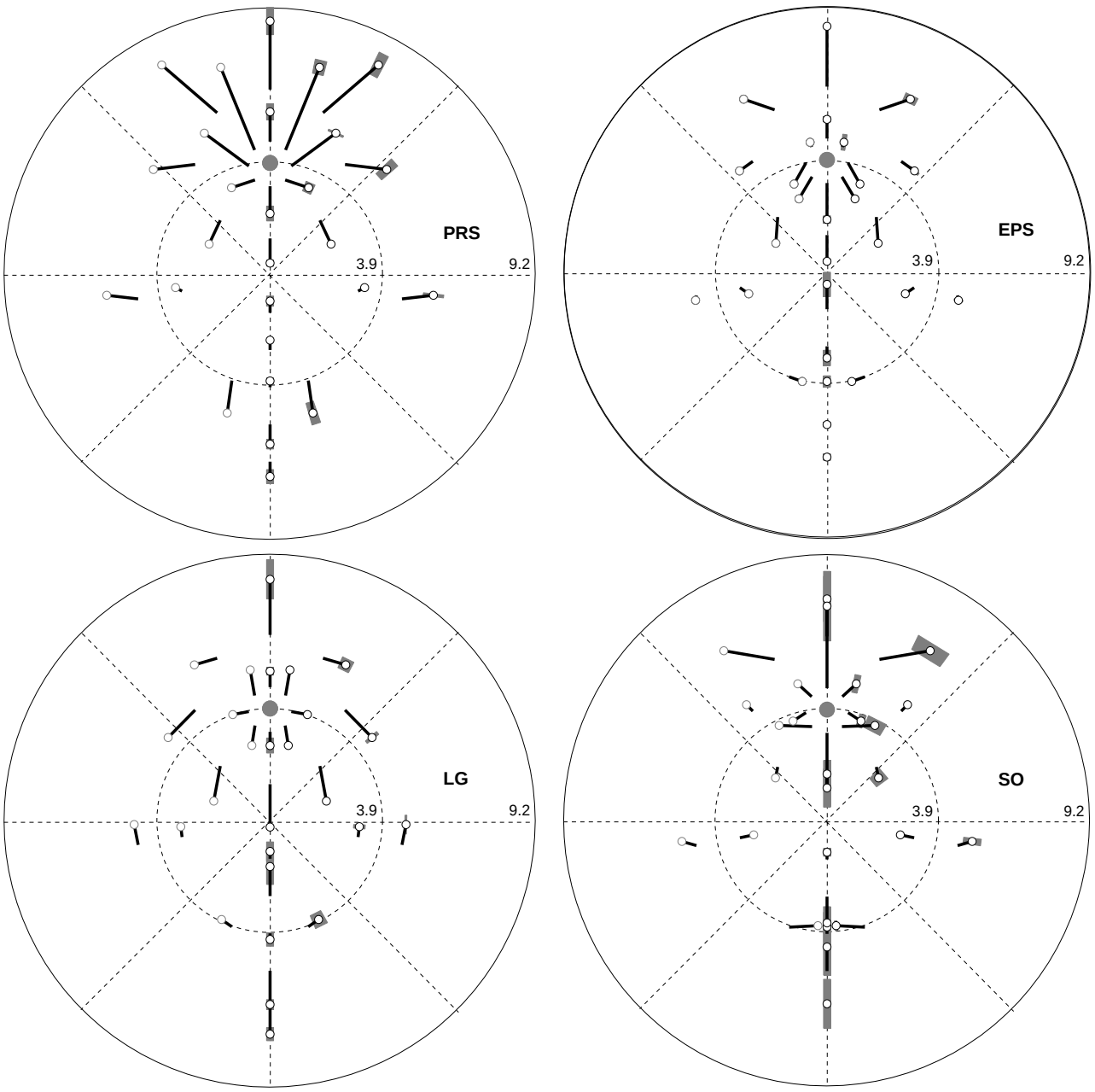

FIGURE 9. Shift in perceived velocity of test dots as a function of their veridical velocity. Each plot shows two-dimensional stimulus velocity, with speed corresponding to distance from the origin. The adaptation stimulus velocity is indicated by the solid grey circle. Shifts are indicated by black line segments, with one end located at the physical test velocity and the other end (indicated by hollow circles) displaced by the shift in perceived velocity due to adaptation. A gray box around each hollow circle indicates the standard error in the speed and DOM measurements. The width of the standard error boxes along the V_y-axis is chosen arbitrarily for visibility. Data were only collected on the right hand side of each plot; shifts plotted on the left side are symmetrically duplicated.

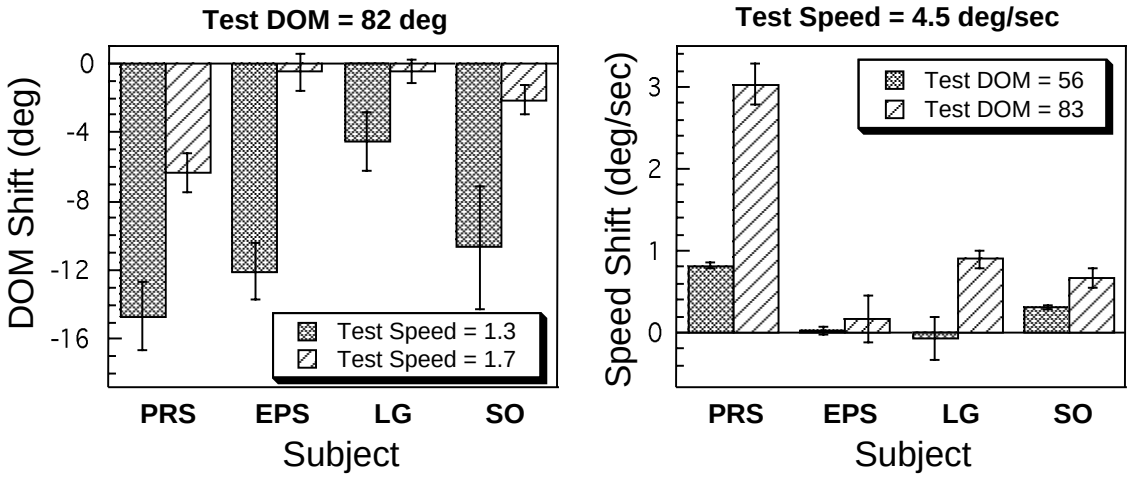

FIGURE 10. Inseparability of velocity shifts with respect to speed and DOM. Data are replotted from Fig. 9, and are shown for each of the four subjects. **Left:** DOM shift for two different test speeds. **Right:** Speed shift for two different test DOMs.

disables a group of neurons tuned for a particular displacement, and subsequent saccadic eye movements are shifted repulsively away from this displacement. The pattern of shifts was interpreted as evidence that these neurons encode the two-dimensional saccadic eye movement targets as a population. These physiological results lend credibility to our hypothesis that the radiating pattern of shifts in perceived velocity might result from a reduction in activity of mechanisms tuned for the adaptation velocity.

Two-dimensional velocity repulsion is a novel finding that could not be inferred from previous results. In addition, the finding of speed repulsion in the present study is interesting, since some previous studies found only speed reduction after adaptation (e.g., Thompson, 1980; Smith, 1985). At least four differences between these studies and our own may explain this discrepancy. First, the previous experiments used sinusoidal or square wave grating stimuli, while we employed dot stimuli. Secondly, previous experiments presented test and match stimuli simultaneously, while ours were temporally separated. Third, our experiments showed a spatio-temporally white noise stimulus at the test location during the adaptation period. This serves to reduce the effect of contrast adaptation on the observed biases, but it may also affect the perceived speed of the test pattern. Finally, previous experiments compared adapted DOM/speed to veridical DOM/speed, while we are comparing to a measurement of the pre-adaptation perceived DOM/speed. The comparison of two motion stimuli in different regions of the visual field need not be veridical. In our unadapted speed discrimination experiments, two of the subjects consistently underestimated the speed of the test stimulus. Such an underestimate would have reduced the match speeds in our experiment, and the resulting speed shifts would have all been negative.

6 Discussion and Conclusions

The results of our experiments are consistent with the theory that the human visual system uses an explicit representation of local image velocities based on a set of mechanisms jointly tuned for speed and DOM. In particular, we have shown that: (1) Shifts in perceived DOM do not show significant spatial frequency tuning, (2) Different adaptation patterns (dots or sinusoidal gratings) with the same perceived velocity produce comparable shifts in test gratings, (3) The shifts in perceived DOM of some test plaid stimuli are opposite those predicted by a STFM adaptation hypothesis, and (4) shifts in perceived speed and DOM are not independent. These results, taken together, are inconsistent with adaptation of STFMs or DSMs, and are consistent with the VM adaptation hypothesis.

This interpretation depends on a number of assumptions. Primarily, we are relying on a simple model of motion adaptation, in which mechanisms selective for the adaptive stimulus are reduced in sensitivity, and this induces subsequent repulsive perceptual shifts that are indicative of the tuning characteristics of those mechanisms. As mentioned in the *Introduction*, this type of assumption has been used in a wide range of psychophysical studies to infer the existence of tuned mechanisms (or "channels"). But alternative explanations (such as changes in tuning properties) have been suggested (e.g., Barlow, 1990).

An important secondary assumption is that adaptation occurs in a *single* encoding site (i.e., within a specific type of mechanism), and that this same mechanism also determines the percept. It is possible that the effects we observe are due to adaptation of several different mechanisms. As discussed previously, multiple adaptation sites may explain the small antipodal DOM repulsion observed in Experiment 1. Furthermore, the different test stimuli used in our experimental conditions may be probing different adaptation sites. Specifically, DOM shifts observed in experiment 3 (using drifting dot test stimuli) may not be directly comparable to those of experiments 1 and 2, which are based on grating test stimuli.

Previous research shows that motion aftereffects depend critically on the choice of test stimulus. The classical MAE, in which a stationary test pattern is seen to move as a result of motion adaptation (see Wade, 1994 for a survey), is substantially different than the effect measured using flickering or moving test stimuli. The stationary MAE is spatial-frequency tuned (Over *et al.*, 1973; Cameron *et al.*, 1992; Ashida & Osaka, 1994) and temporal-frequency tuned (Pantle, 1974). By comparison, the MAE measured with flickering or moving test stimuli is relatively independent of spatial frequency (Ashida & Osaka, 1994) and appears to be tuned for speed (Thompson, 1980; Smith, 1987; Ashida & Osaka, 1995). Several authors have discussed these differences and others, and concluded that the two types of test stimuli are probing the adaptation of different mechanisms (Hiris & Blake, 1992; Nishida & Sato, 1994; Ashida & Osaka, 1994; Ashida & Osaka, 1995). In our experiments, all test stimuli are moving, and thus we might expect our adaptation results

to be independent of spatial frequency. We note, however, that spatial frequency dependencies have been observed in detection threshold elevations for moving gratings (Pantle *et al.*, 1978).

In addition to dependence on the choice of test stimulus, the adaptation site is likely to depend on the choice of adapting stimulus. The data of experiment 1 demonstrate that changing the adapting stimuli from gratings to dots had little effect on DOM shifts, as measured by drifting sinusoidal test stimuli. Nevertheless, it is conceivable that differences would be revealed if one measured two-dimensional velocity shifts using the method of experiment 3. In particular, it would be worthwhile to examine whether grating adaptation produces an elongated pattern of velocity shifts indicative of the velocity constraint line of the grating.

In conculsion, despite the strong assumptions underlying our interpretation, the VM hypothesis seems to provide the most parsimonious explanation of our experimental results. Adaptation-induced perceptual shifts might also be used to probe the representation of more complex motion stimuli. For example, shifts in perceived velocity after adaptation to non-coherent plaids (i.e., plaids in which the components appear to slide over each other) could provide clues as to the representation of multiple motions.

Acknowledgement

We thank Ted Adelson, Mary Bravo, Jacob Nachmias, E.J. Chichilinsky, and David Knill for valuable discussions, and Andrew Smith and a second anonymous reviewer for their helpful suggestions. PRS was supported by NEI Vision Training Grant EY07035-17. The majority of this research was performed while EPS was in the Computer and Information Science Dept, U. Pennsylvania, where he was partially supported by NSF Science and Technology Center Grant SBR-89-20230, and ARO / MURI Grant DAAH04-96-1-0007. EPS is currently supported by the Sloan Foundation through the NYU Theoretical Neurobiology Program, and by NSF CAREER grant 9624855.

References

Adelson, E. H. & Movshon, J. A. (1982). Phenomenal coherence of moving visual patterns. *Nature*, *300*(5892), 523–525.

Albright, T. D. (1984). Direction and orientation selectivity of neurons in visual area MT of the macaque. *J. Neurophysiology*, *52*, 1106–1130.

Ashida, H. & Osaka, N. (1994). Difference of spatial frequency selectivity between static and flicker motion aftereffects. *Perception*, *23*, 1313–1320.

Ashida, H. & Osaka, N. (1995). Motion aftereffect with flickering test stimuli depends on adapting velocity. *Vis. Res.*, *35*(1), 1825–1833.

Barlow, H. B. (1990). A theory about the functional role and synaptic mechanism of visual after-effects. In Blakemore, C., editor, *Vision: Coding and Efficiency*, pages 363–375. Cambridge University Press.

Blakemore, C. B., Nachmias, J., & Sutton, P. (1970). The perceived spatial frequency shift: Evidence for frequency selective neurons in the human brain. *J. Physiol.*, *210*, 727–750.

Blakemore, C. B. & Sutton, P. (1969). Size adaptation: a new aftereffect. *Science*, *166*, 245–247.

Cameron, E. L., Baker, C., & Boulton, J. C. (1992). Spatial frequency selective mechanisms underlying the motion aftereffect. *Vis. Res.*, *32*, 561–568.

Clymer, A. B. (1973). *The effect of seen movement on the apparent speed of subsequent test velocities: speed tuning of movement*. PhD thesis, Columbia University, NY.

Coltheart, M. (1971). Visual feature-analyzers and after-effects of tilt and curvature. *Psychological Review*, *78*, 114–121.

Derrington, A. M. & Suero, M. (1991). Motion of complex patterns is computed from the perceived motions of their components. *Vis. Res.*, *31*, 139–149.

Driver, J., McLeod, P., & Dienes, Z. (1992). Are direction and speed coded independently by the visual system? evidence from visual search. *Vis. Res.*, *6*, 133–147.

Georgeson, M. A. & Harris, M. G. (1984). Spatial selectivity of contrast adaptation: models and data. *Vis. Res.*, *24*, 729–741.

Gibson, J. J. (1950). *The Perception of the Visual World*. Houghton Mifflin, Boston, MA.

Graham, N. (1989). *Visual Pattern Analyzers*. Oxford University Press, New York, NY.

Grzywacz, N. M. & Yuille, A. L. (1990). A model for the estimation of local image velocity by cells in the visual cortex. *Proc. R. Soc. Lond. A*, *239*, 129–161.

Heeger, D. J. (1987). Model for the extraction of image flow. *J. Opt. Soc. Am. A*, *4*(8), 1455–1471.

Hiris, E. & Blake, R. (1992). Another perspective on the visual motion aftereffect. *Proc. Natl. Acad. Sci. USA*, *89*, 9025–9028.

Koenderink, J. J. & van Doorn, A. J. (1990). Affine structure from motion. *J. Opt.*

Soc. Am. A, *8*, 377–385.

Lee, C., Rohrer, W. H., & Sparks, D. L. (1988). Population coding of saccadic eye movements by neurons in the superior colliculus. *Nature*, *332*, 357.

Levinson, E. & Sekuler, R. (1976). Adaptation alters perceived direction of motion. *Vis. Res.*, *16*, 779–781.

Lew, A. C., Song, E. Y., Friedman-Hill, S. R., Adelson, E. H., & Wolfe, J. M. (1991). A different aftereffect of motion: altering perceived direction of gratings and plaids. In *Investigative Opthalmology and Visual Science Supplement (ARVO)*, volume 32, page 827.

Loomis, J. M. & Nakayama, K. (1973). A velocity analogue of brightness contrast. *Perception*, *2*, 425–428.

Mather, G. (1980). The movement aftereffect and a distribution-shift model for coding the direction of visual movement. *Perception*, *9*, 379–392.

Maunsell, J. H. R. & Essen, D. C. V. (1983). Functional properties of neurons in middle temporal visual area of the macaque monkey I. Selectivity for stimulus direction, speed, and orientation. *Journal of Neurophysiology*, *49*, 1127–1147.

Movshon, J. A., Adelson, E. H., Gizzi, M. S., & Newsome, W. T. (1986). The analysis of moving visual patterns. In Chagas, C., Gattass, R., & Gross, C., editors, *Experimental Brain Research Supplementum II: Pattern Recognition Mechanisms*, pages 117–151. Springer-Verlag, New York.

Movshon, J. A. & Newsome, W. T. (1996). Visual response properties of striate cortical neurons projecting to ar ea MT in macaque monkeys. *Visual Neuroscience*, *16*(23), 7733–7741.

Murakami, I. & Shimojo, S. (1993). Motion capture changes to induced motion at higher luminance contrasts, smaller eccentricities and larger inducer sizes. *Vis. Res.*, *33*, 2091–2107.

Nishida, S. & Sato, T. (1994). Motion aftereffect with flickering test patterns reveals higher stages of motion processing. *Vis. Res.*, *35*(4), 477–490.

Nowlan, S. J. & Sejnowski, T. J. (1995). A selection model for motion processing in area MT of primates. *J. of Neuroscience*, *15*, 1195–1214.

Osgood, C. E. & Heyer, A. W. (1952). A new interpretation of the figural after-effect. *Psychology Rev.*, *59*.

Over, R., Broerse, J., Crassini, B., & Lovegrove, W. (1973). Spatial determinants of the aftereffects of seen motion. *Vis. Res.*, *13*, 1681–1690.

Pantle, A. (1968). Size-detecting mechanisms in human vision. *Science*, *162*, 1146–1148.

Pantle, A. (1974). Motion aftereffect magnitude as a measure of the spatio-temporal response properties of direction-sensitive analyzers. *Vis. Res.*, *14*, 1229–1236.

Pantle, A., Lehmkuhle, S., & Caudill, M. (1978). On the capacity of directionally selective mechanisms to encode different dimensions of moving stimuli. *Per-*

ception, *7*, 261–267.

Press, W. H., Flannery, B. P., Teukolsky, S. A., & Vetterling, W. T. (1988). *Numerical Recipes in C*. Cambridge University Press, New York.

Rodman, H. R. & Albright, T. D. (1987). Coding of visual stimulus velocity in area MT of the macaque. *Vis. Res.*, *27*, 2035–2048.

Ross, J. & Speed, H. D. (1991). Contrast adaptation and contrast masking in human vision. *Proc. R. Soc. Lond. B*, *246*, 61–69.

Schrater, P. & Simoncelli, E. (1995). Biases in speed perception due to motion aftereffect. In *Investigative Opthalmology and Visual Science Supplement (ARVO)*, volume 36, pages S–54.

Schrater, P. & Simoncelli, E. P. (1994). Motion adaptation effects suggest an explicit representation of velocity. In *Investigative Opthalmology and Visual Science Supplement (ARVO)*, volume 35, page 1268.

Sekuler, A. B. (1990). Motion segregation from speed differences: Evidence for nonlinear processing. *Vis. Res.*, *30*, 785–795.

Sekuler, R., Pantle, A., & Levinson, E. (1978). Physiological basis of motion perception. In Held, R., Leibowitz, H. W., & Teuber, H., editors, *Handbook of Sensory Physiology VIII, Perception*, pages 67–96. Springer-Verlag, New York.

Sereno, M. E. (1993). *Neural computation of pattern motion: modeling stages of motion anaysis in the primate visual cortex*. MIT Press, Cambridge, MA.

Simoncelli, E. P. (1993). *Distributed Analysis and Representation of Visual Motion*. PhD thesis, Massachusetts Institute of Technology, Dept of Electrical Engineering and Computer Science, Cambridge, MA.

Simoncelli, E. P. & Heeger, D. J. (1998). A model of neuronal responses in visual area MT. *Vision Research*, *38*(5), 743–761.

Smith, A. T. (1985). Velocity coding: Evidence from perceived velocity shifts. *Vis. Res.*, *27*, 1491–1500.

Smith, A. T. (1987). Velocity perception and discrimination: Relation to temporal mechanisms. *Vis. Res.*, *27*, 1491–1500.

Smith, A. T. & Edgar, G. K. (1994). Antagonistic comparison of temporal frequency filter outputs as a basis for speed perception. *Vis. Res.*, *34*, 253–265.

Smith, A. T. & Hammond, P. (1985). The pattern specificity of velocity aftereffects. *Exp. Brain Res.*, *60*, 71–78.

Snowden, R. J. (1994). Adaptability of the visual system is inversely related to its sensitivity. *J. Opt. Soc. Am. A*, *11*, 25–32.

Sutherland, N. S. (1961). Figural after-effects and apparent size. *Quarterly J. Expt. Psych.*, *13*, 222–228.

Thompson, P. (1980). Velocity after-effects: The effects of adaptation to moving stimuli on the perception of subsequently seen moving stimuli. *Vis. Res.*, *21*, 337–345.

Wade, N. J. (1994). A selective history of the study of visual motion aftereffects. *Perception*, *23*, 1111–1134.

Warren, W. H. & Hannon, D. J. (1988). Direction of self-motion is perceived from optical flow. *Nature*, *336*, 162–163.

Watson, A. B. & Ahumada, A. J. (1983). A look at motion in the frequency domain. In Tsotsos, J. K., editor, *Motion: Perception and representation*, pages 1–10. Association for Computing Machinery, New York.

Watson, A. B. & Pelli, D. G. (1983). QUEST: A Bayesian adaptive psychophysical method. *Perception & Psychophysics*, *33*, 113–120.

Yang, Y. & Blake, R. (1994). Broad tuning for spatial frequency of neural mechanisms underlying visual perception of coherent motion. *Nature*, *371*, 793–796.